RESTRICTED INVESTIGATION REPORT 1237R

CSIRO

INSTITUTE OF EARTH RESOURCES

DIVISION OF MINERAL PHYSICS

RELATIONSHIP BETWEEN MAGNETIC FABRIC AND GEOLOGICAL STRUCTURE IN THE NORTHERN LEASES AREA, BROKEN HILL

D.A. CLARK

P.O. Box 136,
NORTH RYDE. NSW
AUSTRALIA. 2113

JULY, 1981.

RESTRICTED INVESTIGATION REPORT 1237R

RELATIONSHIP BETWEEN MAGNETIC FABRIC AND GEOLOGICAL STRUCTURE IN THE NORTHERN LEASES AREA, BROKEN HILL

D.A. CLARK

Division of Mineral Physics
P.O. Box 136,
NORTH RYDE. NSW 2113

JULY, 1981.

INDEX

		Page
1.	INTRODUCTION	1
2.	SUSCEPTIBILITY ANISOTROPY AND MAGNETIC FABRIC	2
3.	EXPERIMENTAL PROCEDURE	4
4.	CORRELATION BETWEEN PETROFABRIC AND MAGNETIC FABRIC	6
5.	CONCLUSIONS	15
6.	REFERENCES	16
7.	FIGURE CAPTIONS	17

LIST OF TABLES

TABLE 1	SAMPLING PROGRAMME
TABLE 2	SUSCEPTIBILITY ANISOTROPY
TABLE 3	STRUCTURE AND MESOSCOPIC FABRIC
TABLE 4	MAGNETIC FABRIC

1. INTRODUCTION

The work described in this report was carried out as part of the CSIRO-AMIRA Rock Magnetism Project 78/P96, which has the aim of investigating applications of rock magnetism to mineral exploration. During the course of this project the susceptibility anisotropy of many rock formations has been studied and in most cases a correlation with regional geological structure was apparent. In particular, samples from the Redan area south of Broken Hill collected in the course of a proprietary project for North Broken Hill Ltd. showed a well-developed magnetic fabric.

Because of the structural complexity of the Broken Hill Block and the lack of detailed mapping in the Redan area, it was suggested that a study of the relationship between magnetic fabric, microscopic petrofabric, and mesoscopic and regional structure be carried out in the Northern Leases area, where detailed mapping and extensive structural petrological work have successfully resolved many stratigraphic and structural problems (Laing et al., 1978; Marjoribanks et al., 1980).

The aim of this study is to examine the correlation between magnetic fabric and geological structure in the relatively well-understood Northern Leases area, and to evaluate the applicability of magnetic fabric studies as an aid to structural mapping in other parts of the Broken Hill Block where the structure is not so well known.

The advantage of magnetic fabric determination over conventional methods is the ease with which large areas can be sampled and the rapidity with which large numbers of samples can be processed. Structural petrology by comparison is tedious and time-consuming. In addition very faint fabrics can often be detected by magnetic methods which are invisible in the field and would only be revealed in microscopic studies by counting very large numbers of grain orientations. The principal disadvantage of the magnetic method is that an average fabric attributable to all the magnetic grains in a specimen is determined, whereas detailed microscopic examination may reveal the presence of several superposed fabrics, which in many cases can be

related to specific geological events by their association with different mineralogical assemblages.

In summary, therefore, the magnetic approach and conventional techniques should be viewed as complementary - magnetic fabric studies allowing wide coverage, and structural petrology providing very detailed information on the relationship between rock fabric and geological history, which can then be used to interpret the magnetic fabric data.

2. SUSCEPTIBILITY ANISOTROPY AND MAGNETIC FABRIC

A review of the principles and applications of magnetic fabric studies has been given by Clark and Embleton (1980). The points relevant to the present study will be summarised here.

When the magnetic grains in a rock specimen exhibit a preferred alignment, the measured susceptibility of the specimen depends on the direction of the applied field. This anisotropy of susceptibility can be represented, as an aid to visualisation, by an ellipsoid. The major axis of the susceptibility ellipsoid is the susceptibility measured along the easiest direction of magnetisation (i.e. the maximum susceptibility is along the major axis of the ellipsoid). The intermediate and minor axes of the ellipsoid lie in the plane normal to the major axis, and are perpendicular to each other. The minor axis is parallel to the hardest direction of magnetisation (minimum susceptibility) and the intermediate axis corresponds to the maximum susceptibility within the plane normal to the major axis.

The magnetic lineation is defined to be parallel to the major susceptibility axis. The magnetic foliation is the plane containing the major and intermediate susceptibility axes, and is therefore a plane of high susceptibility. The magnetic foliation pole is normal to the foliation plane, and therefore corresponds to the minor susceptibility axis.

Magnetic fabric arises from two main causes, depending on the type of magnetic grains in the rock.

(i) Shape anisotropy of titanomagnetite or titanomaghaemite grains. The cubic magnetic minerals are intrinsically isotropic in low magnetic fields. However inequidimensional grains of these highly magnetic minerals exhibit strong shape anisotropy due to self-demagnetisation of the grain. This means that magnetite grains, for instance, are more easily magnetised along the long axis of the grain than along a short axis. Therefore if cubic ferrimagnetic minerals are responsible for the susceptibility of the rock, the magnetic fabric reflects preferred orientation of long and short axes of inequidimensional grains.

(ii) Magnetocrystalline anisotropy of titanohaematite or pyrrhotite grains. Minerals of lower symmetry than cubic exhibit strong intrinsic anisotropy. In haematite and pyrrhotite the susceptibility within the basal plane (001) is much greater than the susceptibility along the c-axis [001]. If these minerals dominantly contribute to the susceptibility of the rock, the magnetic fabric reflects preferred crystallographic orientation.

The dominant magnetic carrier in the Northern Leases samples is believed to be magnetite, implying the observed magnetic fabric is a grain-shape fabric.

The magnitude of susceptibility anisotropy is quantified by a number of parameters which can be used to characterise the magnetic fabric:

$$\text{Anisotropy } A = k_{max}/k_{min}$$
$$\text{Lineation } L = k_{max}/k_{int}$$
$$\text{Foliation } F = k_{int}/k_{min}$$
$$\text{Prolateness } P = L/F$$

If the fabric is dominantly planar parallel (foliation dominant) then $P < 1$ and the susceptibility ellipsoid is oblate. If the fabric is dominantly linear parallel (lineation dominant) then $P > 1$ and the susceptibility ellipsoid is prolate.

A number of studies of the magnetic fabric of deformed and metamorphosed rocks have produced similar results. While the magnetic fabric accurately parallels any visible mesoscopic fabric in rocks, it

often reveals a fabric element which was otherwise undetectable. In most cases the axes of the susceptibility ellipsoid are parallel to the principal strain axes, with maximum susceptibility (magnetic lineation) along the direction of maximum extension, and minimum susceptibility (magnetic foliation pole) along the direction of maximum compression. The magnetic foliation is therefore analogous to slaty cleavage and metamorphic foliation.

Overprinting of fabrics is commonly observed in high grade metamorphic rocks and this will be reflected in the magnetic fabric. Therefore the presence of two non-parallel foliations in a rock will result in a magnetic foliation plane lying between the two foliations, plus a magnetic lineation along the intersection of the foliation planes. Similarly the presence of two lineations will produce a resultant magnetic lineation lying between the two, plus a magnetic foliation plane containing the lineations. If the rock has a lineation which lies out of the foliation plane, the resultant magnetic fabric will consist of a foliation lying between the true foliation and the lineation, containing a lineation along the projection of the true lineation onto the foliation plane.

Because the degree of overprinting is likely to be inhomogeneous, the resultant magnetic fabric will vary according to which petrofabric component is dominant. In favourable circumstances this can enable determination of the fabric components present. Conversely, well-grouped magnetic lineations and foliation poles from a site strongly suggest that only a single fabric is present.

To extract most information from the magnetic fabric data, the values of the parameters A, L, F and P should be considered along with the purely directional data.

3. EXPERIMENTAL PROCEDURE

Samples were collected either with a portable field drill or in the form of small blocks from 22 sites in the Northern Leases areas. All samples were oriented using both sun-compass and magnetic compass bearings and the orientations are accurate to within 2° Details of the

sampling are given in Table 1 and the sampling localities are shown in Figure 1.

Data from a previous field trip to the Broken Hill region are also included in this report. A banded-iron formation near Imperial Ridge in the Northern Leases is labelled site 23; samples from the Redan area are collectively known as "site" 24 and are included for comparison with the Northern Leases.

A number of cylindrical specimens (2.5 cm diameter, 2.2 cm height) were cut from each of the samples and the susceptibility ellipsoid for each specimen was determined using a Digico anisotropy spinner, after the bulk susceptibility of the specimen had been measured on a Digico bulk susceptibility bridge. Data on bulk susceptibility and the various anisotropy parameters are summarised in Table 2.

Because most of the samples are weakly magnetic and only slightly anisotropic, the anisotropy signal is very weak and must be integrated over a large number of revolutions. Accurate determination of the anisotropy of the weakest specimens required about 8 minutes per specimen. Reduction of the measurement time by a factor of 4 doubles the noise and for many specimens introduced significant random errors into the measurement. However, when all specimens from a site were considered the overall pattern of susceptibility axis directions was very similar whether 2 minutes or 8 minutes per specimen was used for measurement. When working with very weakly magnetic rocks either long measurement times per specimen or statistical analysis of measurements of large numbers of specimens must be used.

The results demonstrate the success of magnetic fabric studies using the above instrumentation on rocks as weak as the granite gneiss (sites 5-9) which has average susceptibility of 48×10^{-6} and an anisotropy of only about 3%. This corresponds to a difference in (emu) susceptibility along the major and minor axes of 1.4×10^{-6}. The noise level specified by the manufacturer for 256 revolutions per axis (each specimen is spun about 3 perpendicular axes), which corresponds to about 2 minutes measurement time, is 0.01×10^{-6}. Stipulating that the minimum susceptibility difference between major and minor axes of 10 times the noise level is desirable, specimens with bulk susceptibility

of 10 x 10^{-6} and 1% anisotropy (i.e. A = 1.01) can be processed at the rapid rate of 30 per hour. Specimens weaker than this possess sufficiently few magnetic grains (assuming the susceptibility carrier is magnetite and the specimen volume is about 11 cm^3) that statistical fluctuations in grain alignment will produce large errors in determination of the fabric from any one specimen. The only solution to this problem is measuring large numbers of specimens, or specimens larger in volume, to average out statistical departures from the mean fabric.

4. CORRELATION BETWEEN PETROFABRIC AND MAGNETIC FABRIC

Table 3 summarises the mesoscopic fabric elements observed at the sampling sites, and their structural context. Table 4 lists the magnetic fabric elements determined from the susceptibility anisotropy measurements. Figures 2-12 are equal area plots of principal susceptibility axis directions from sites or goups of sites, together with data on bedding, mesoscopic schistosities and lineations, and fold axes.

Sites 1-4 (Figure 2)

Sites 1-4 in Potosi gneiss are from near the hinge of the Mine antiform. The bulk susceptibility of the samples is variable, but overall rather high, and some specimens have susceptibilities greater than 1,000 x 10^{-6}, which is comparable to fresh basalts. This fact and the high degree of anisotropy, averaging 24%, imply that the susceptibility anisotropy is very easily measurable.

Remembering that magnetic fabric elements are undirected lines and that therefore antiparallel points on the net are strictly equivalent, it can be seen from Figure 2 that the major, intermediate and minor susceptibility axes are all well-grouped. For convenience all points are plotted on the lower hemisphere of the net. Lineation directions, for instance, which are approximately 180° in declination away from the main group must be reversed for calculating mean directions in which case they fall on the upper hemisphere of the net.

From the diagram the magnetic foliation poles (minor susceptibility axes) plunge shallowly to the south, and the magnetic lineations are directed east, also with shallow plunge. The mean magnetic foliation pole and the mean magnetic lineation lie very close to the pole to observed S_2 schistosity and the plunge of the F_2 fold respectively.

In this case there is very good agreement between the magnetic fabric elements and the known structural elements. The value of prolateness 0.95 suggests that the fabric is predominantly oblate, i.e. in the field of flattening. This is consistent with the lack of a visible mineral lineation.

Site 5-9 (Figures 3 and 4)

These sites form a continuation of the traverse from the hinge of the Mine antiform (site 1) to the NW limb. In a number of places bedding (S_o) and bedding-parallel schistosity (S_1) were visible as well as the cross-cutting S_2 schistosity. Therefore, in contrast to the hinge zone, there is overprinting of fabrics and it is to be expected that the magnetic fabric will be more complex, and interpretation correspondingly more difficult.

From the diagrams it can be seen that the magnetic fabric shows partial rotational symmetry about an axis defined by clustering of lineations with NE plunges. The minor and intermediate susceptibility axis directions are dispersed around a girdle perpendicular to the mean lineation. Within this girdle the minor and intermediate axes are not intermixed, but are each confined to separate sections of the girdle. The magnetic foliation poles are streaked along the arc between the S_2 pole and the S_1 pole determined at site 6. This is precisely what is expected from inhomegeneous overprinting of S_1 by S_2. The observed foliation pole will be between the S_1 and S_2 poles, lying closer to whichever pole corresponds to the stronger schistosity.

The observed magnetic lineation lies along the intersection of the two schistosities, which is sub-parallel to the fold axis. Note that the principal susceptibility axis directions of a few specimens are anomalous. In most cases the major and intermediate axes or the

intermediate and minor axes are interchanged. This is quite commonly observed in magnetic fabric data and reflects inhomogeneous response to deformation with varying degrees of overprinting (see Clark and Embleton (1980), Figure 4.2). The gross fabric remains apparent from the overwhelming majority of susceptibility axis directions, but more definite resolution of the fabric elements can often be achieved by considering susceptibility ellipsoid shape as well as axis directions.

Although precise estimates of schistosity poles cannot be obtained from the magnetic data, as was possible for sites 1-4, the plot of susceptibility axes indicates the presence of non-parallel overprinted schistosities, and suggests the two schistosity poles have shallow plunge to the south and moderate plunge to the west respectively (i.e. the schistosities are approximately E-W with steep dip to the north, and N-S with moderate dip to the east). This agrees reasonably well with the mapped mesoscopic schistosities. The mean magnetic lineation is quite well defined (with an error of 15°) and gives an estimate of the plunge of F_2 (approximately 55° to the ENE). Thus the essential structural information contained in the mapped fabric elements is also revealed in the magnetic fabric.

This example illustrates the importance of collecting samples from several sites in an area of overprinted fabrics. The susceptibility ellipsoids of individual specimens represent an averaged fabric with consequent loss of information. Thus it is necessary to sample extensively, obtaining sufficient variation in degree of overprinting to resolve the component fabrics.

Sites 10-18 (Figures 5 and 6)

The Lord's Hill granite gneiss is very weakly magnetic with average emu susceptibility 18 x 10^{-6}, but the relatively large anisotropy of around 10% enables the susceptibility ellipsoids of specimens to be readily determined.

The principal susceptibility axis directions from all specimens are plotted in Figure 5. Although plotted directions appear to fill most of the net, the distribution of major and minor axes is far from random.

Major axes are concentrated in the NE quadrant and minor axes are mostly clustered about a sub-horizontal N-S direction, with some streaking towards a westerly direction with moderate plunge. Overall the fabric is reminiscent of sites 5-9. This is not surprising since sites 10-18 exhibit S_1 and S_2 schistosties with similar orientations to those found at sites 5-9.

A considerable clarification is achieved by plotting only the major axes from specimens with lineation dominant ($P > 1$) and only the minor axes from those with dominant foliation ($P < 1$). The resultant fabric diagram (Figure 6) is much more clear-cut. Magnetic lineations, with one exception, are well-grouped in the NE quadrant close to the F_2 fold plunge at site 13, which is given by the intersection of S_1 and S_2 in Figure 6. The mean magnetic lineation is also sub-parallel to the mesoscopic L_{1-2} which has somewhat variable plunge within S_2. In the case of the anomalous specimen 17A, the major and intermediate axes are simply interchanged.

The magnetic foliation poles are mostly well-clustered about the S_2 schistosity pole, implying that S_2 is the dominant schistosity along this traverse. However, specimen 14A has interchanged intermediate and minor axes, reflecting the dominant S_1 schistosity at site 14. Overall the magnetic fabric shows well-grouped principal axes, with major axes parallel to the fold axis and mesoscopic lineation, minor axes parallel to the S_2 schistosity pole, and intermediate axes parallel to the S_1 schistosity pole from site 14, which is fortuitously orthogonal to the S_2 pole.

The simplicity of Figure 6 compared to Figure 5 illustrates the advantage of taking ellipsoid shape (that is, relative values of L and F) into account when plotting scattered data. In many cases interpretation is greatly assisted by considering only the well-defined fabric elements from each specimen.

Site 19 (Figure 7)

Three samples were collected in this amphibolite unit. Sample 19A shows planar fabric with $P < 1$ for all specimens and grouping of minor axes with major and intermediate axes dispersed around a girdle

perpendicular to the magnetic foliation poles. In contrast samples 19B and 19C have a well-defined linear fabric. In general $P \geq 1$ for specimens from the latter samples and the major axes are well-grouped, whilst the intermediate and minor axes are more dispersed about the great circle perpendicular to the magnetic lineation, which also contains the S_2 pole.

The minor axes, however, are not clustered about the S_2 schistosity pole and in fact are biased away from it within the girdle. For each sample the magnetic foliation poles are quite well-grouped, but the between-sample variation is much greater. The samples are separated by a few metres, so the variation in attitude of the magnetic foliation is on mesoscopic scale.

It is suggested that the magnetic foliation represents a folded S_1 schistosity which is not readily observed in the outcrop, and which defines an mesoscopic F_2 fold plunging shallowly to the SW, parallel to the well-defined magnetic lineations and the plunge of the macroscopic F_2 synform.

Again, consideration of ellipsoid shape simplifies the interpretation and increases confidence in conclusions drawn from the data.

Site 20 (Figure 8)

Only two specimens were obtained from this site which is in sillimanite-biotite-garnet gneiss, close to the hinge of an F_2 synform plunging at approximately 45° to the SW. Only a single layer-parallel schistosity is visible.

Any conclusions based on only two specimens must be tentative, but the magnetic foliation poles appear to be consistent with the mapped S_{1-2} schistosity pole. The magnetic lineations do not agree well with the fold axis direction, but the significance of this is not clear in the absence of information on the statistical scatter of directions.

Site 21 (Figure 9)

Site 21 was within the same unit as site 20, but S_2 oblique to S_1 was visible. Magnetic foliation poles are well-grouped in the SE quadrant, and magnetic lineations appear to be randomly dispersed within the corresponding foliation plane. Intermediate axes, which are omitted from the Figure for clarity, are intermingled with the major axes within the magnetic foliation plane. For one specimen (21B6) intermediate and minor axes are interchanged.

Because the S_1 and S_2 schistosities are almost parallel (only 15° apart) it is difficult to determine whether the magnetic foliation pole corresponds closest to S_1 or S_2 poles. The mean magnetic foliation pole is 16° from the S_2 pole and 24° from the S_1 pole, suggesting that S_2 is dominantly reflected in the magnetic fabric.

The scatter of magnetic lineations would allow no deduction of direction of maximum extension from the magnetic fabric data alone. When the magnetic lineations from site 20 are considered in the light of the data from site 21 which has similar fabric, it can be seen that the discordance between the magnetic lineations and the fold axis is not statistically significant.

Site 22 (Figures 10 and 11)

The sericite schist samples from site 22 in the Globe-Vauxhall shear zone are very weakly magnetic, but have relatively strong anisotropy, averaging 11%. The magnetic fabric is very well-developed in most specimens.

In Figure 10 principal susceptibility axes of all specimens are plotted and it is evident that minor axes are clustered in the SW quadrant with shallow plunges and that major and intermediate axes form two distinct groups, sub-vertical and sub-horizontal, within the steeply dipping magnetic foliation plane. The magnetic lineations are predominantly sub-vertical but in several specimens the major and intermediate axes are interchanged. In all cases the lineations of these anomalous specimens are weak ($L < 1.02$).

In Figure 11 major axes of specimens with $L \geq 1.02$ and minor axes of specimens with $F \geq 1.02$ are plotted. It is immediately apparent that the magnetic fabric is better defined by this approach, which takes ellipsoid shape into account. The magnetic lineation plunges very steeply to the NW, and the scatter in magnetic foliation poles has been reduced. The mean magnetic foliation pole is (124°, +19°), defining a magnetic foliation plane striking N34°E, dipping 71° to the NW. Because the shear zone dips to the SE, the magnetic foliation is oblique to the boundaries of the shear, although they have the same strike. The magnetic foliation is parallel to the well-developed S_3 schistosity visible in the samples and is presumably characteristic of the fabric in the retrogressed rocks in the vicinity of the Globe-Vauxhall shear. The magnetic lineation appears to parallel the L_3 lineation which is related to the direction of movement along the shear.

Site 23

A BIF unit at Imperial Ridge had been sampled previous to the present study and the magnetic fabric data are included for comparison. The susceptibility anisotropy of banded rocks with highly magnetic layers is often due to textural anisotropy. This arises from self-demagnetisation of highly magnetic layers, which consequently are more easily magnetised in the plane of the layer than perpendicular to it. These rocks therefore have a plane of high susceptibility (magnetic foliation) parallel to the layering.

Eight samples were drilled from the one outcrop in which the compositional banding, which is presumably S_0, showed mesoscopic folding. The magnetic foliation poles from all specimens are well-grouped about (128°, +54°) and with one exception are parallel to the bedding poles. In the anomalous sample the magnetic foliation was consistent with the overall magnetic foliation, but was strongly oblique to S_0 which had been folded to a different orientation. This suggests that the magnetic foliation in fact represents an S_{1-2} which is mostly, but not always, bedding-parallel. A corollary is that the magnetic fabric arises from preferred orientation of inequidimensional magnetite grains, rather than from textural anisotropy.

The mean magnetic lineation is not very well-defined but appears to have shallow plunge to the WSW, consistent with L_{1-2}. Further sampling of BIF units is required to elucidate the structural significance of magnetic fabric in this rock type.

Redan Area (Figure 12)

A number of quartz-magnetite, Redan gneiss and amphibolite units from widely dispersed localities in the Redan area have been sampled in the course of a previous study, and the magnetic fabric is discussed here for comparison with the results from the Northern Leases.

Overall the magnetic foliation planes of rock units from the Redan area strike roughly NE and dip steeply to the NW. This is consistent with the predominantly S_2-parallel magnetic fabric found in the Northern Leases, but cuts across the regional E-W trends of rock units in the Redan area. The magnetic lineations are also scattered but steep NW plunges predominate. In the absence of petrofabric studies in this area, the significance of the magnetic fabric is unknown.

Discussion

The origin of the magnetic fabric in the gneissic rocks and amphibolites is uncertain, but is probably due to preferred orientation of long axes of magnetite grains. This is the most plausible explanation for the fabric of the rock samples with relatively high susceptibilities (sites 1-4 and site 19). Shape anisotropy of magnetite grains is also the preferred explanation for the fabric of the BIF unit. However, in other rock types, such as granitic gneiss and sericite schist, the very low susceptibility may be due to paramagnetic rock-forming minerals alone. Ferromagnesian minerals such as biotite, amphiboles and pyroxenes have emu susceptibilities typically around 50 x 10^{-6} and are intrinsically anisotropic. Therefore strong preferred orientation of these minerals may account for the observed susceptibility anistropy of some of the Broken Hill rocks. It would be of value to resolve the question of the origin of the susceptibility anisotropy, possibly by rock magnetic experiments.

Whatever the origin of the susceptibility anisotropy, it is apparent that magnetic fabric is very well correlated with mesoscopic fabric and structure in the Northern Leases area. In all cases a well-defined magnetic fabric is found which can be related to the mesoscopic structural elements. When both well-defined lineations and foliations are observed in the magnetic data they are in good agreement with corresponding mesoscopic structures (sites 1-4, 10-18 and 22). In some cases the magnetic fabric exhibits axial symmetry (sites 19, 20-21). The axis of symmetry, lineation or foliation pole, then coincides with the fold axis or dominant schistosity pole, respectively. In this latter case the complementary fabric element (axial-plane schistosity, or lineation) cannot be determined from the magnetic fabric alone.

In a locality exhibiting significant overprinting of petrofabrics (sites 5-9) the nature of the overprinting and the approximate orientation of the intersecting schistosities was apparent from the magnetic fabric. The plunge of F_2 was well estimated by the mean magnetic lineations.

When the magnetic fabric diagrams are compared with the plots of mapped structural elements from the various sub-areas (Laing et al., 1978, Figure 7), the correspondence is remarkable. The correlation between the magnetic fabric and the mapped structural elements is summarised below:

Site Nos.	Subarea (Laing et al., (1978)	Correlation
1-9	Broken Hill Antiform (near subarea 3)	Magnetic lineation = L_{1-2} and F_2 plunge. Strong magnetic foliation = S_2 Weak magnetic foliation = S_0/S_1
10-18	North Mine (subarea 3)	Magnetic lineation = L_{1-2} and F_2 plunge Magnetic foliation ($P < 1$) = S_2

Site Nos.	Subarea (Laing et al., (1978)	Correlation
19	Round Hill (subarea 5)	Magnetic lineation = L_{1-2} and F_2 plunge Magnetic foliation = S_0/S_1
20-21	E of Round Hill (subarea 6)	Magnetic foliation = S_2
22	Globe-Vauxhall shear (adjacent to sub-areas 5 and 7)	Strong magnetic lineation = L_3 Magnetic foliation = S_3 (subarea 7)
23	SE of Imperial Ridge (subarea 6)	Magnetic lineation = L_{1-2} Magnetic foliation = S_{1-2}

5. CONCLUSIONS

(i) The magnetic susceptibility anisotropy of a number of different lithologies exhibiting a variety of structural features has been investigated. In all cases the sampled rocks exhibit a well-developed magnetic fabric. The feasibility of determining the magnetic fabric of these lithologies; which are well-represented in the Broken Hill area and which range from highly magnetic (BIF) to very weakly magnetic (granitic gneiss and sericite schist); has been demonstrated.

(ii) In all cases the magnetic fabric accords well with the known petrofabric. The correlation is so clear that in most cases it is felt that useful information on the structure could be inferred from the magnetic fabric alone. This suggests that the magnetic method could be usefully applied to areas where the geological structure is not as well known, extrapolating relationships between magnetic fabric and structure found in nearby areas. The overall relationships found to apply in the Northern Leases (except in retrograde schist zones) are that mean magnetic lineation, if defined, is consistent with mesoscopic lineation and F_2 fold plunge; magnetic foliation poles, if well-grouped, are

parallel to the pole to axial-plane S_2, or if streaked around a great circle arc, reflect variable overprinting of S_0/S_1 by S_2. It has not been established whether magnetic lineation dominantly reflects L_2 or F_2 plunge parallel to L_1, if these are oblique. Sampling at a locality where L_2 oblique to L_1 is present should resolve this question. In the Globe-Vauxhall shear zone the magnetic fabric coincides with the $S_3 + L_3$ petrofabric.

(iii) The ease and rapidity of the magnetic method, which makes it an ideal tool for reconnaissance mapping or very detailed studies of a small area, is illustrated by the present study, which involved one day's sampling and two days' laboratory work.

(iv) The magnetic fabric of an individual specimen represents an average of the petrofabric components present. It has been demonstrated in the course of this work that this disadvantage of the magnetic method can be largely overcome by adequate sampling of the rock unit to obtain sufficient variation in degree of overprinting. Magnetic fabric studies however, can never be substituted for detailed mapping or microscopy but should be regarded as complementary to conventional techniques, ideally suited to extrapolation or interpolation of known relationships.

(v) Maximum information is extracted from magnetic fabric data if the susceptibility ellipsoid shapes are considered in conjunction with orientation diagrams of susceptibility axis direction. For the final interpretation in terms of structure all available geological information should be integrated with the magnetic data.

6. REFERENCES

D.A. Clark and B.J.J. Embleton (1980), "Applications of Rock Magnetism to Mineral Exploration", CSIRO Restricted Investigation Report 1193R.

W.P. Laing, R.W. Marjoribanks and R.W.R. Rutland (1978), Econ. Geol., 73, 1112-1136.

R.W. Marjoribanks, R.W.R. Rutland, R.A. Glen and W.P. Laing (1980), Precamb. Res., 13, 209-240.

7. FIGURE CAPTIONS

Figure 1 — Sampling localities in the Northern Leases.

Figures 2-12 — Magnetic fabric orientation diagrams. Equal-area (Schmidt net) lower hemisphere projections based on the true north. The primitive represents the present horizontal. Major susceptibility axes (magnetic lineations) are represented by squares, intermediate susceptibility axes by triangles (sometimes omitted for clarity), and minor susceptibility axes (magnetic foliation poles) are plotted as dots. Estimated schistosity planes, their corresponding poles, mesoscopic lineations and fold axis plunges are also indicated.

Figure 2 — Magnetic fabric orientation data from sites 1-4.

Figure 3 — Magnetic fabric orientation data from sites 5-9 with measured schistosity and bedding poles.

Figure 4 — Magnetic lineations and foliation poles from sites 5-9. Bedding and mesoscopic schistosity planes also shown.

Figure 5 — Magnetic fabric orientation data of all specimens from sites 10-18.

Figure 6 — Sites 10-18. Magnetic lineations from specimens with prolate susceptibility ellipsoids, magnetic foliation poles from specimens with oblate ellipsoids. Anomalous directions from specimens 14A and 17A are labelled.

Figure 7 — Magnetic fabric orientation data from site 19. Directions from samples 19A, 19B and 19C are labelled.

Figure 8 — Magnetic fabric orientation data from site 20.

Figure 9 — Magnetic fabric orientation data from site 21. Anomalous directions from specimen 21B6 are labelled.

Figure 10 — Magnetic fabric orientation data of all specimens from site 22.

Figure 11 — Site 22 magnetic lineations of specimens with $L \geq 1.02$, magnetic foliation poles of specimens with $F \geq 1.02$.

Figure 12 — Magnetic lineations and foliation poles from the Redan area.

TABLE 1 SAMPLING PROGRAMME

Site Nos.	No. of Samples	Rock Type	Locality
1-9	20	Potosi gneiss	Mine antiform east of Thompson shaft. Traverse from hinge of F2 structure to NW limb.
10-18	19	Granite gneiss	Hangingwall synform defined by Lord's Hill granite gneiss.
19	3	Amphibolite	SE limb of Round Hill synform, SW of Round Hill shaft
20-21	3	Sillinanite-biotite-garnet gneiss	F_2 synform SE of Silver Peak shaft
22	2	Sericite schist	Globe-Vauxhall shear zone at Silver Peak shaft.
23*	8	Banded iron formation	SE of Imperial Ridge
24*	32	Quartz-magnetite; Redan gneiss: Amphibolite	Redan area

* "Sites" 23 and 24 were sampled in July, 1979. Sites 1-22 were sampled in March, 1981.

TABLE 2 SUSCEPTIBILITY ANISOTROPY

Site Nos.	No. of specimens	$\bar{k}$ (Range)	$\bar{A}$	$\bar{L}$	$\bar{F}$	$\bar{P}$
1-4	9	650 (20-2,290)	1.24 ± 0.04	1.08 ± 0.02	1.14 ± 0.03	0.95 ± 0.03
5-9	20	48 (23-106)	1.03 ± 0.01	1.02 ± 0.01	1.01 ± 0.01	1.00 ± 0.003
10-18	35	18 (9-35)	1.10 ± 0.02	1.05 ± 0.01	1.05 ± 0.01	1.01 ± 0.01
19	9	170 (140-260)	1.06 ± 0.01	1.03 ± 0.01	1.03 ± 0.01	1.00 ± 0.01
20-21	19	40 (26-95)	1.06 ± 0.02	1.04 ± 0.02	1.02 ± 0.004	1.01 ± 0.02
22	18	28 (9-48)	1.11 ± 0.03	1.02 ± 0.01	1.09 ± 0.02	0.94 ± 0.02
23	8	18,000 (1,800-38,100)	1.21	1.08	1.12	0.96
24	69	Very variable, depending on lithology				

$\bar{k}$ = mean emu susceptibility x 10^6. The range of values for individual specimens from the site(s) is given in parentheses.

$\bar{A}$ = mean anisotropy

$\bar{L}$ = mean lineation magnitude

$\bar{F}$ = mean foliation magnitude

$\bar{P}$ = mean prolateness

Mean values are quoted ± standard error

TABLE 3 STRUCTURE AND MESOSCOPIC FABRIC

Site	Mapped structure and fabric
1	On limb of possible F_2 drag structure defined by folded pegmatite segregation and cross-cutting S_2 (Hinge zone of F_2 Mine antiform).
3	S_2 schistosity visible
4	Small scale drag folds defined by pegmatite segregations S_2 axial plane schistosity visible, dipping $\sim 70^{\circ}$ to NW (towards NW limb of Mine antiform).
6	In core of F_2 drag fold plunging at 44° to $N77^{\circ}E$ S_2 dominant schistosity-striking $N77^{\circ}E$ S_1 in hinge-striking $\sim N15^{\circ}E$.
7	Well-developed S_2.
8	S_2 dominant schistosity. F_2 plunging 40° to $N72^{\circ}E$
9	S_2 as for site 8, strike $N72^{\circ}E$, dip 70° to NW. S_o striking $N127^{\circ}E$, dipping 15° to NE. (on NW limb of Mine antiform).
10-12	Dominant S_2 axial plane schistosity strike $N72^{\circ}E$, dip 70° to NW. L_{1-2} plunging 24° - 47° to NE within S_2.
13	Mesoscopic F_2 fold hinge, plunge 25 - 30° to NE. Both S_1 // S_o and S_2 are well developed. S_1 strikes $N167^{\circ}E$, dips 46° to E.
14	S_1 dominant.
15-18	S_2 dominant.

19 SE limb of Round Hill F_2 synform, plunging $\sim 20^{\circ}$ to SW.
Axial plane S_2 striking N37°E, dipping 65° to NW.

20 Close to hinge of F_2 synform, plunging around 45° to SW.
Schistosity is probably S_2 but is layer parallel.
S_{1-2} strikes N7°E, dips 54° to W.

21 $S_1//S_o$ and S_2 are both visible.
Bedding: strike N17°E, dips 35° to W.
S_2: strike $\sim$ NE, dip $\sim 40^{\circ}$ to NW.

22 Globe-Vauxhall shear zone. S_3 schistosity visible.

23 S_o visible.

TABLE 4 MAGNETIC FABRIC

Site Nos.	Magnetic lineation (α_{95})	Magnetic foliation pole (α_{95})
1-4	(84°, $+21^{o}$) (16°)	(178°, $+20^{o}$) (12°)
5-9	(72°, $+55^{o}$) (15°)	--
10-18	(65°, $+49^{o}$) (16°)	(164°, $+3^{o}$) (18°)
19	(213°, $+33^{o}$) (10°)	--
20	--	(106°, $+25^{o}$) (--)
21	--	(129°, $+34^{o}$) (9°)
22	(328°, $+69^{o}$) (8°)	(124°, $+19^{o}$) (5°)
23	(250°, $+20^{o}$) (46°)	(128°, $+54^{o}$) (20°)
24	(324°, $+63^{o}$) (43°)	(97°, $+21^{o}$) (39°)

NOTES:

(i) Directions are quoted in the form (declination, inclination) with the convention that declination is positive clockwise from north and inclination is positive downwards.

For example a lineation direction (84°, $+21^{o}$) corresponds to a plunge of 21° to N84^{o}E. A foliation pole (178°, $+20^{o}$) corresponds to a foliation plane (which by definition is normal to the pole) which strikes N88^{o}E and dips 70° to N358^{o}E (N2^{o}W).

(ii) Mean directions are calculated assigning unit weight to specimens. α_{95} is the radius of the 95% circle of confidence about the mean direction, assuming the directions follow a Fisher distribution.

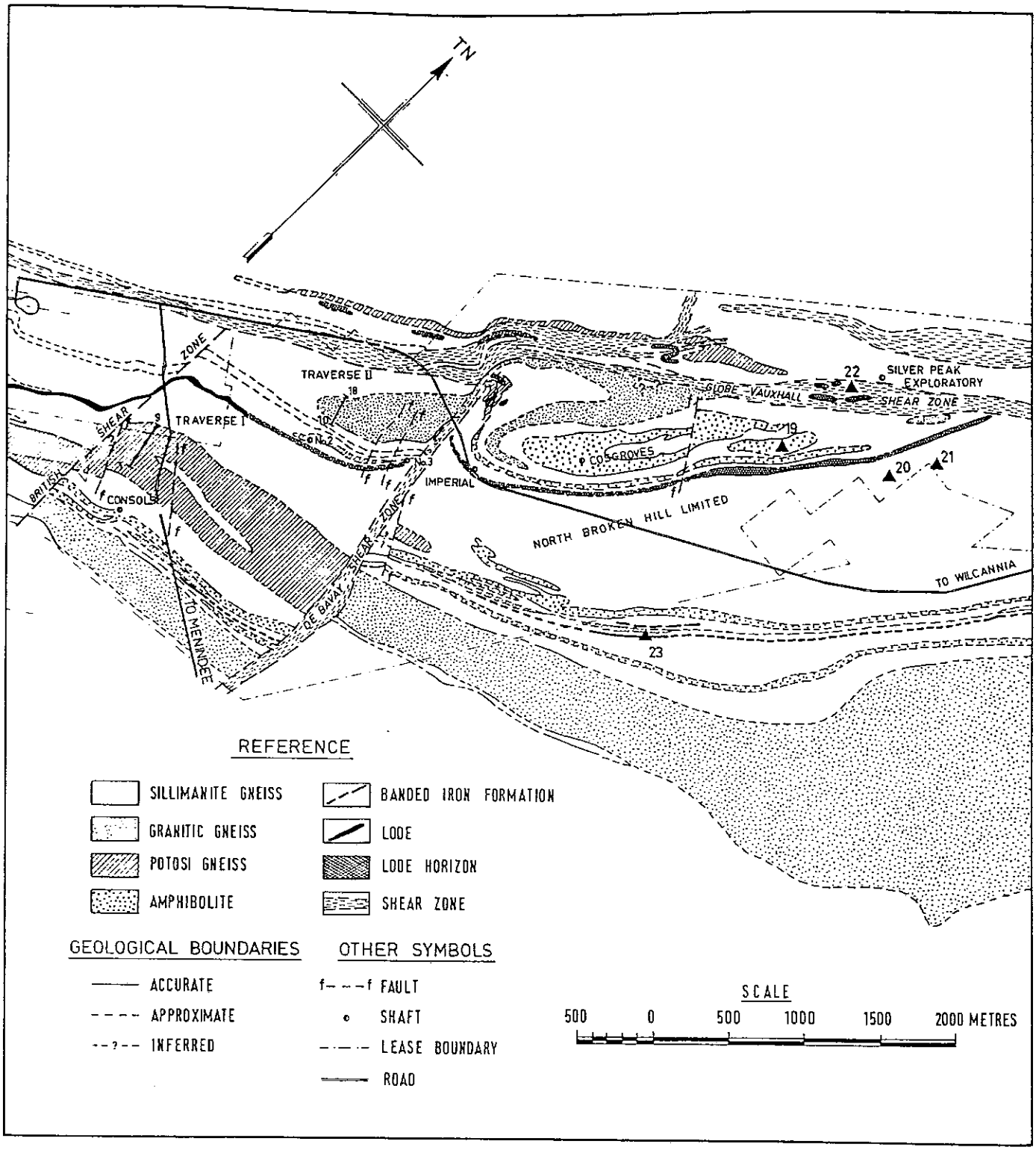
TN
TRAVERSE II
TRAVERSE I
SHEAR ZONE
BRITISH
CONSOLS
IMPERIAL
No.2
No.3
COSGROVES
GLOBE VAUXHALL
SHEAR ZONE
SILVER PEAK EXPLORATORY
22
19
20
21
23
NORTH BROKEN HILL LIMITED
TO WILCANNIA
TO MENINDEE
DE BAVAY SHEAR ZONE
REFERENCE
SILLIMANITE GNEISS
GRANITIC GNEISS
POTOSI GNEISS
AMPHIBOLITE
BANDED IRON FORMATION
LODE
LODE HORIZON
SHEAR ZONE
GEOLOGICAL BOUNDARIES
ACCURATE
APPROXIMATE
INFERRED
OTHER SYMBOLS
FAULT
SHAFT
LEASE BOUNDARY
ROAD
SCALE
500 0 500 1000 1500 2000 METRES

FIG. 1

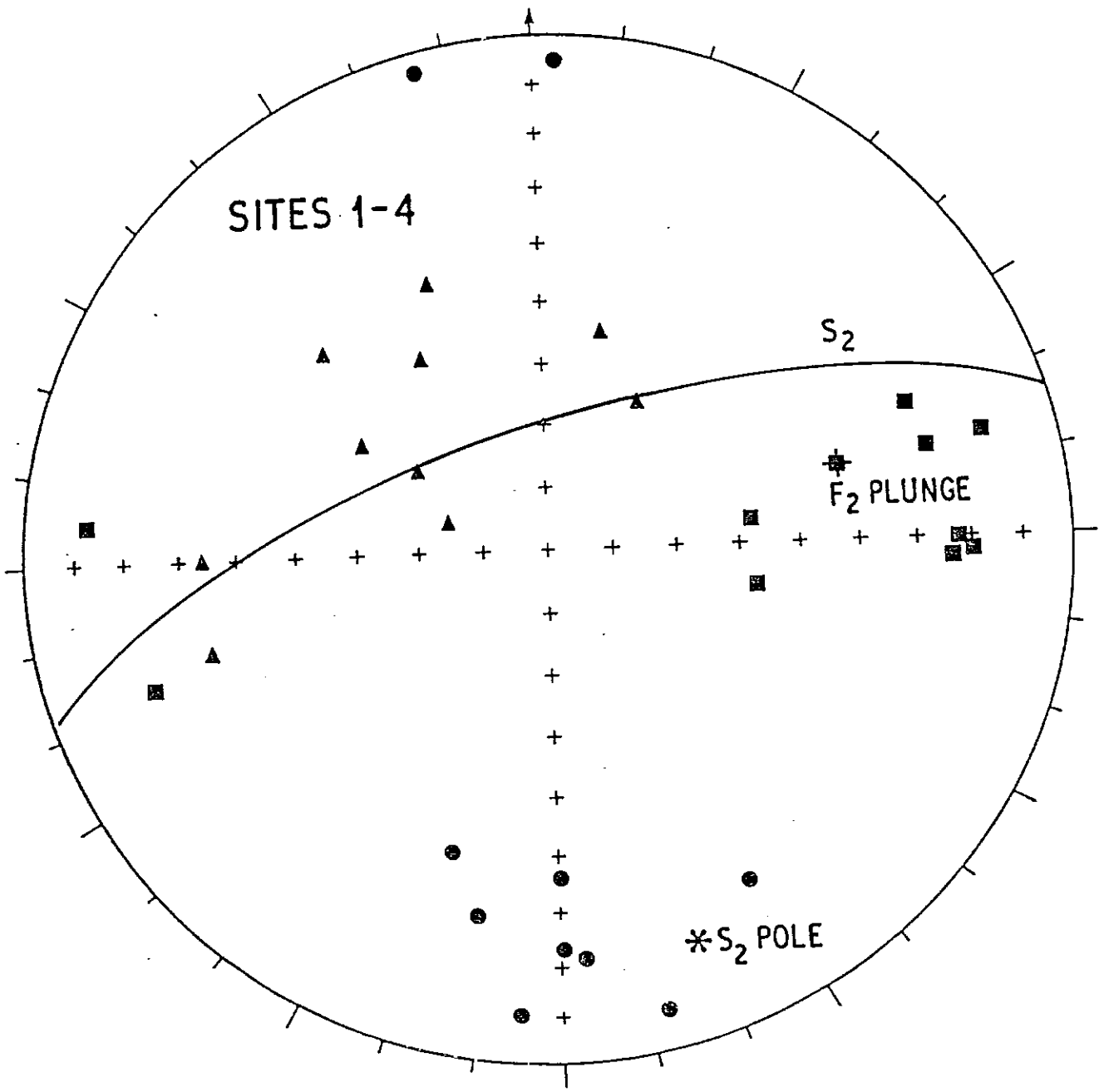

FIG. 2

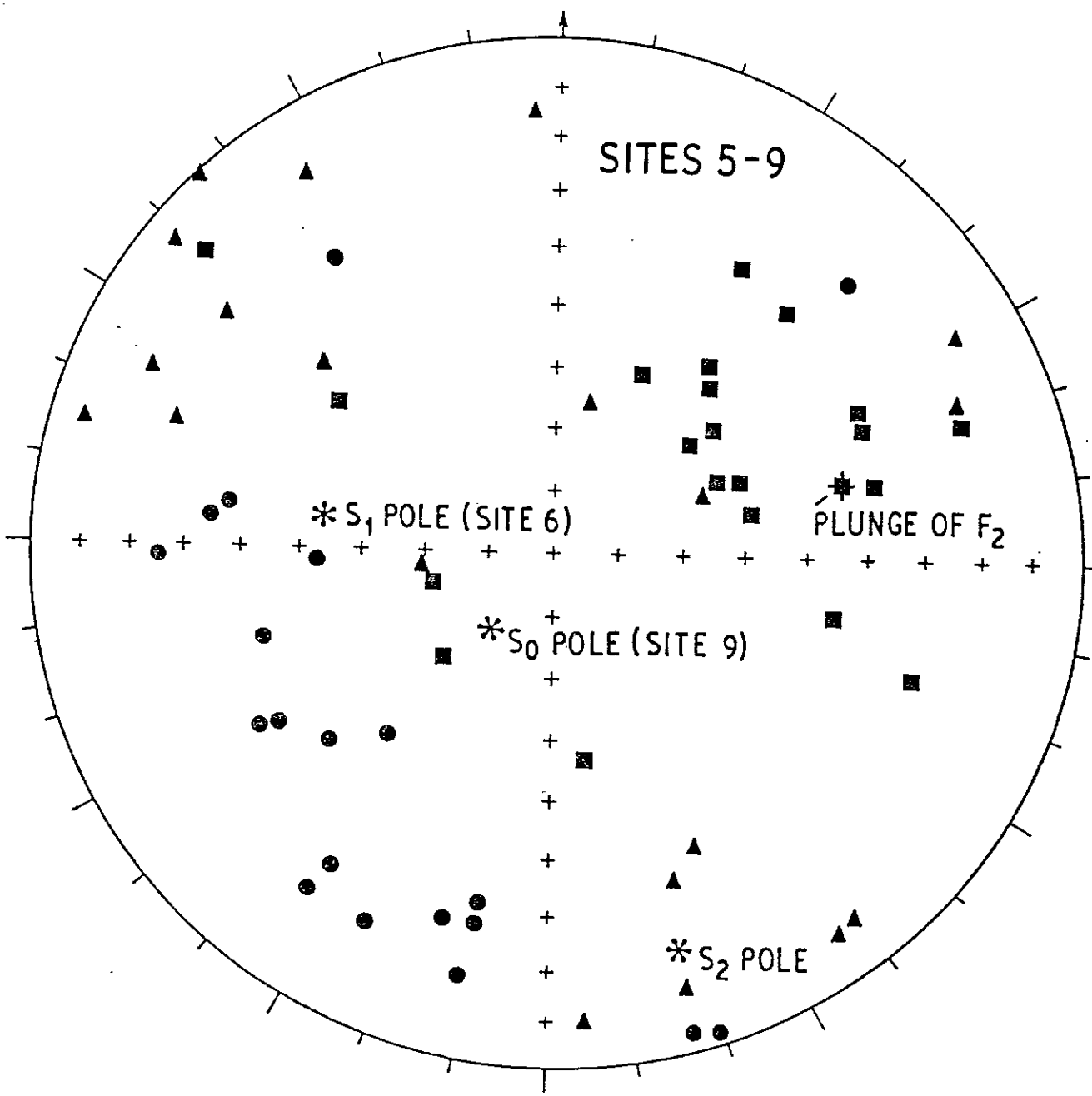

FIG. 3

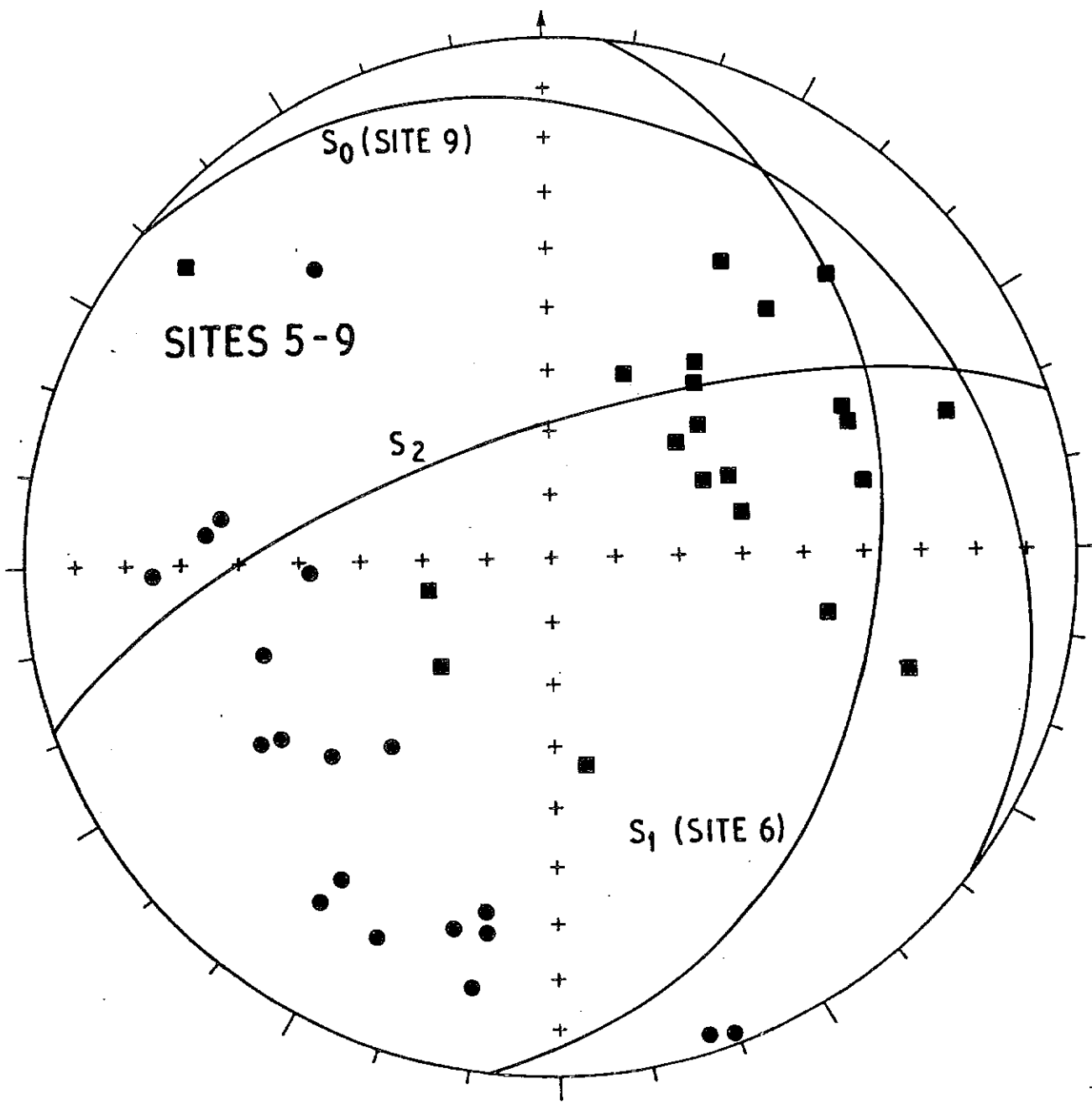

FIG. 4

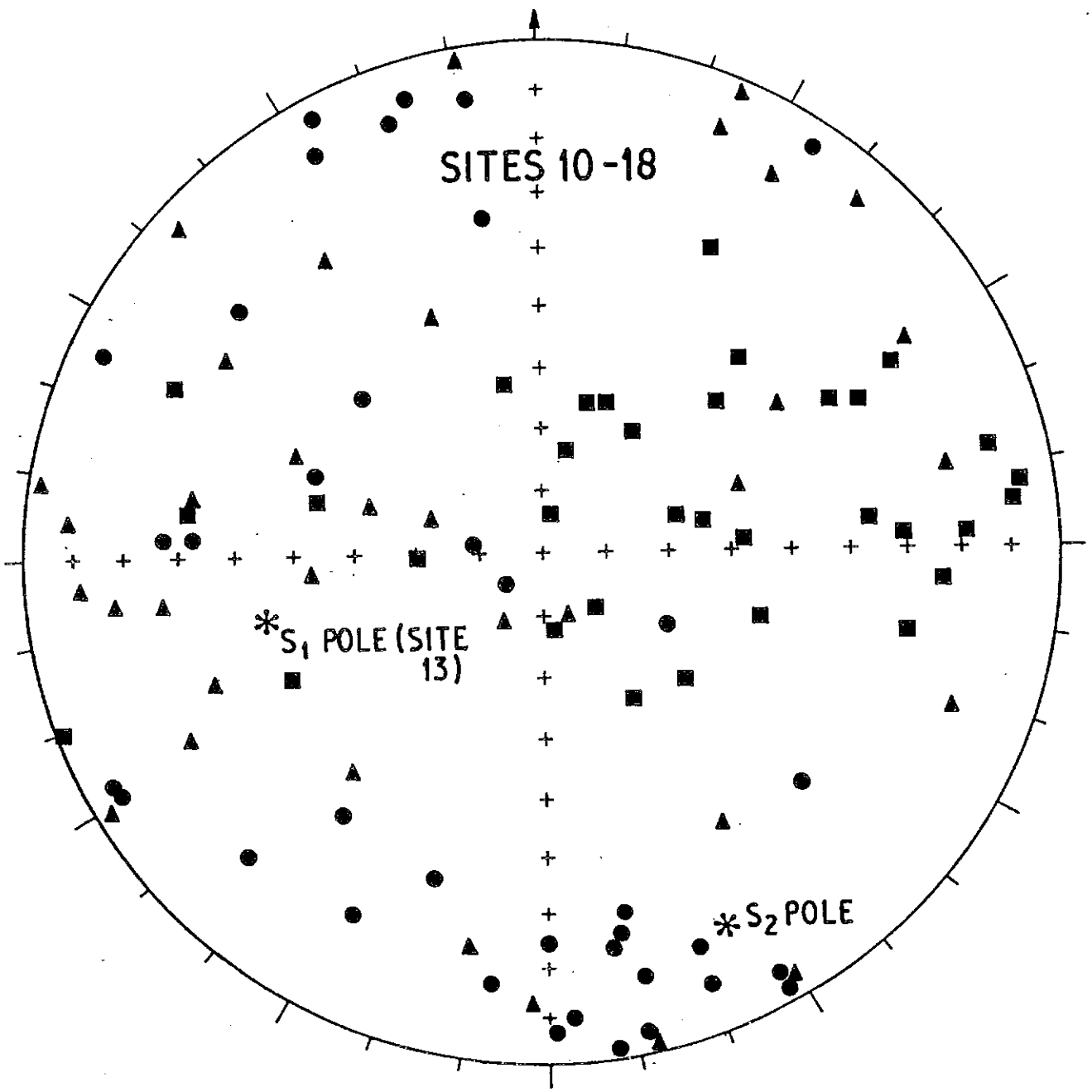

FIG. 5

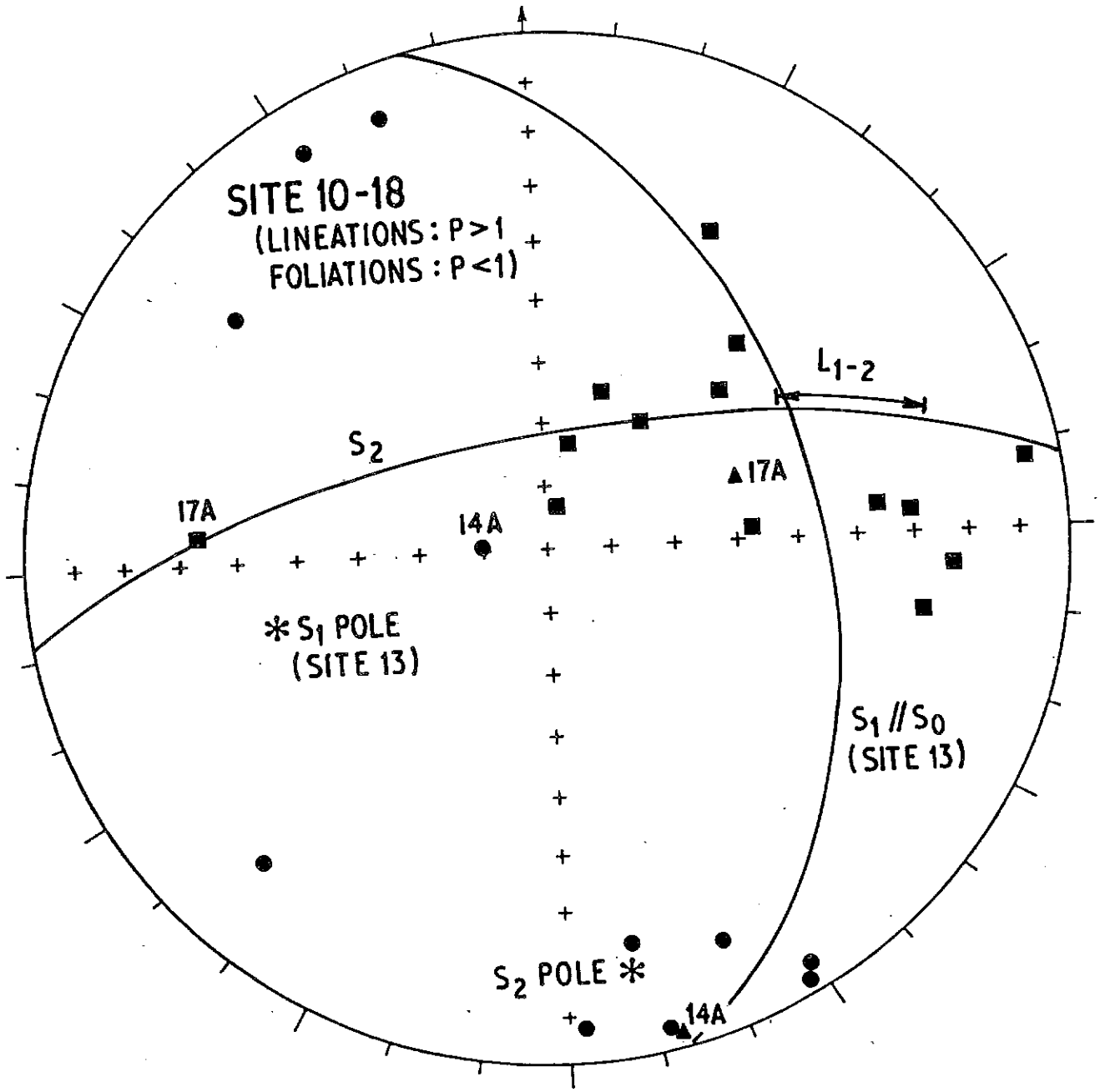
SITE 10-18
(LINEATIONS : P>1
FOLIATIONS : P<1)
L_{1-2}
S_2
17A
14A
17A
* S_1 POLE
(SITE 13)
$S_1 // S_0$
(SITE 13)
S_2 POLE *
14A

FIG. 6

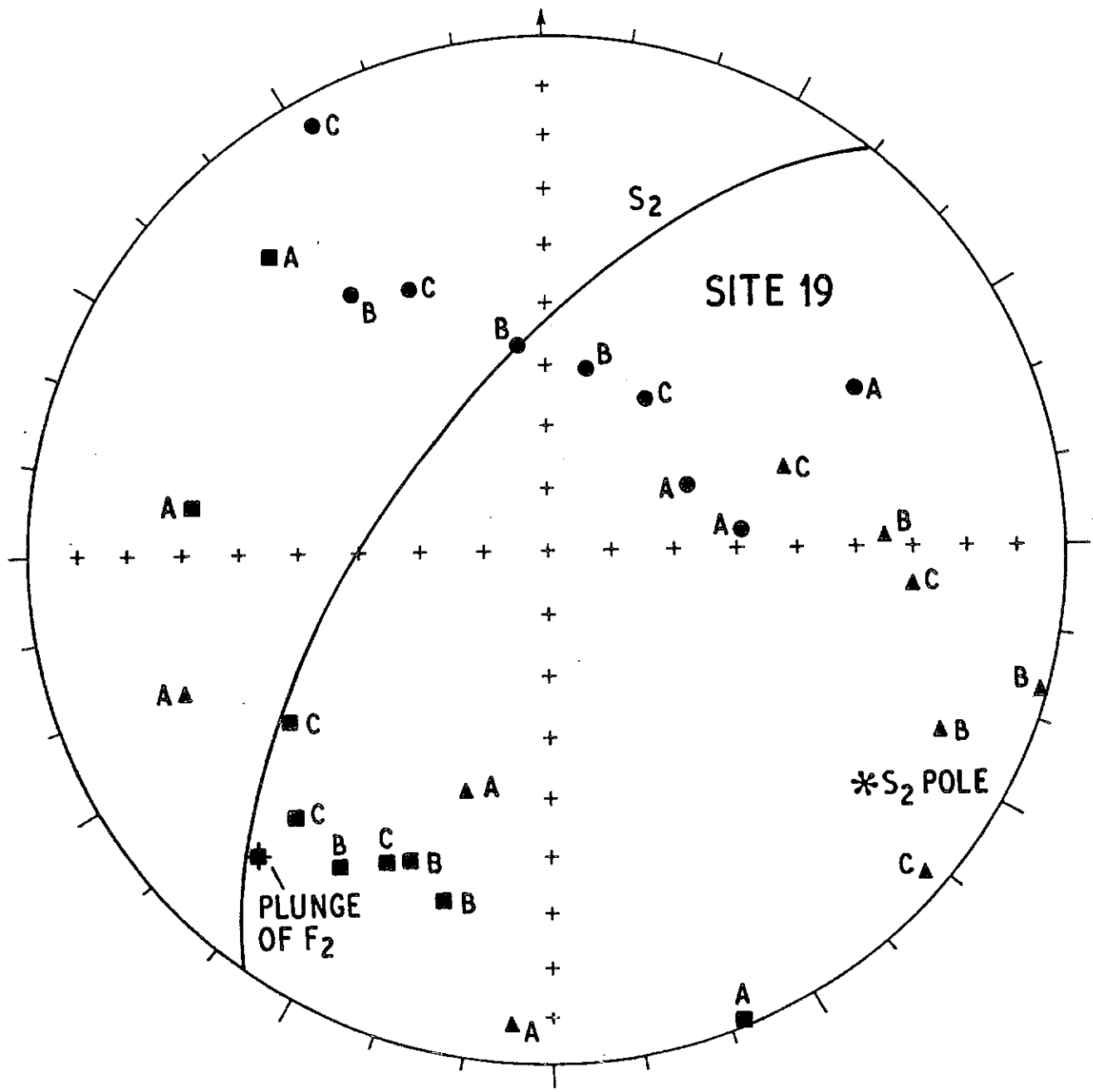

FIG.7

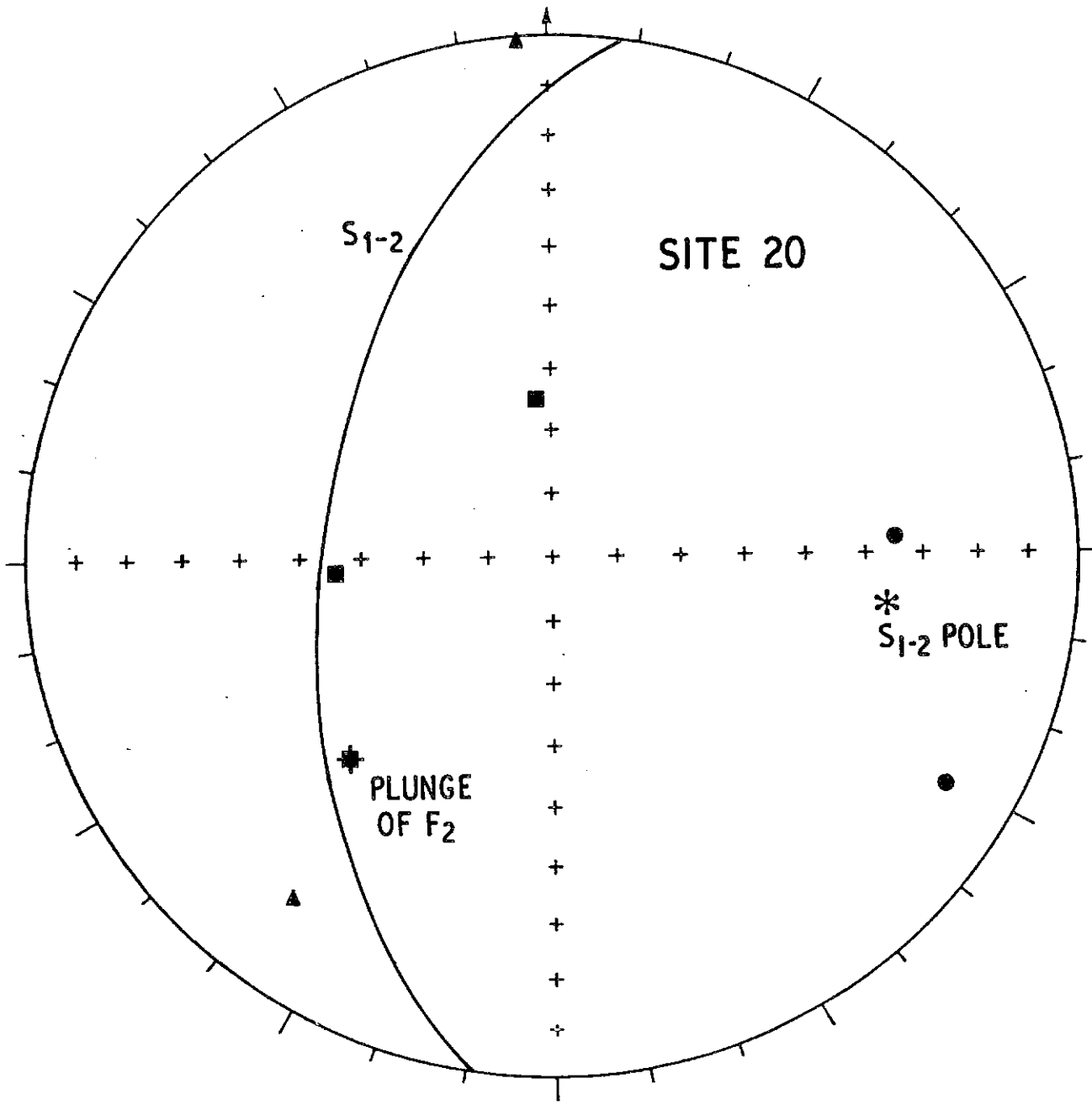

FIG. 8

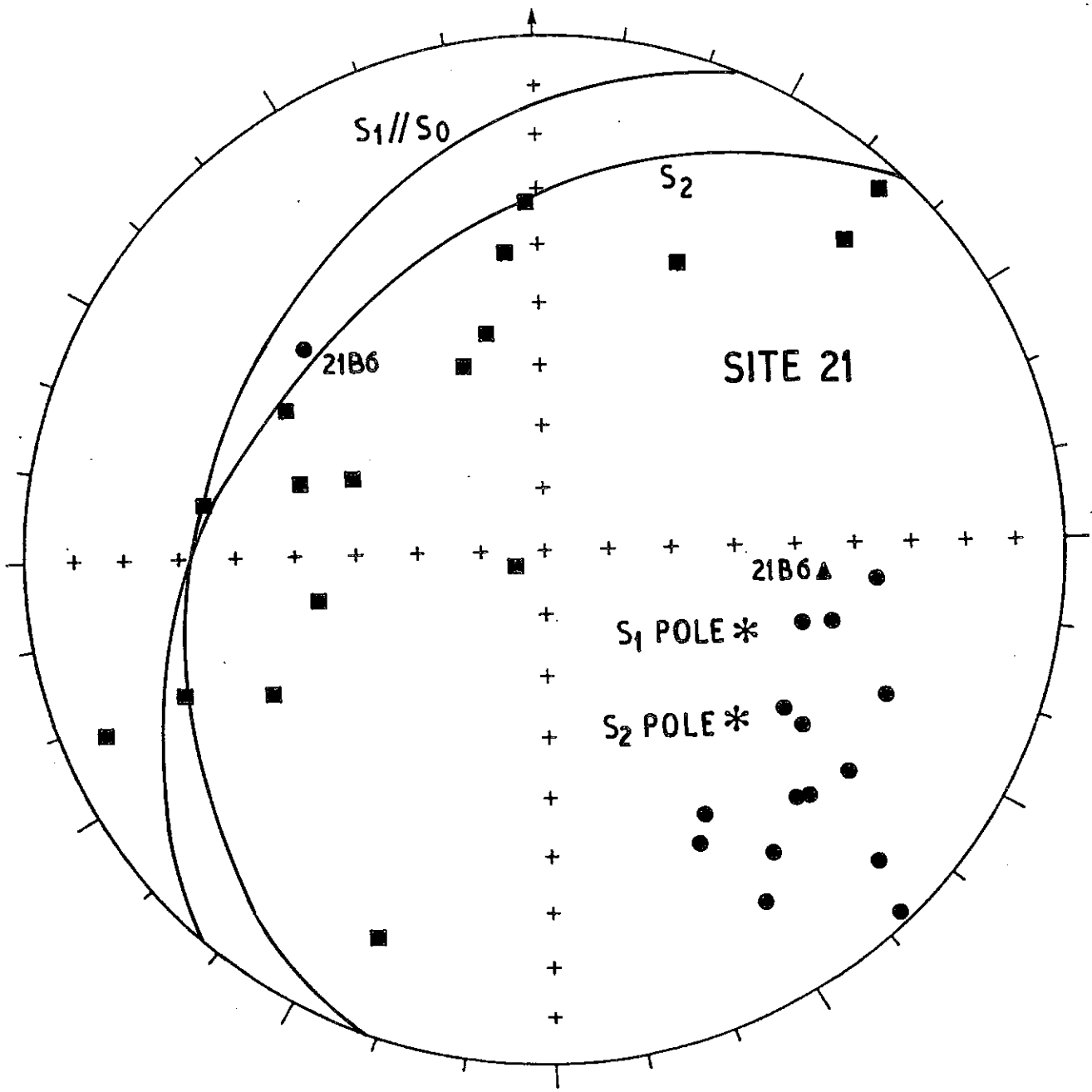

FIG. 9

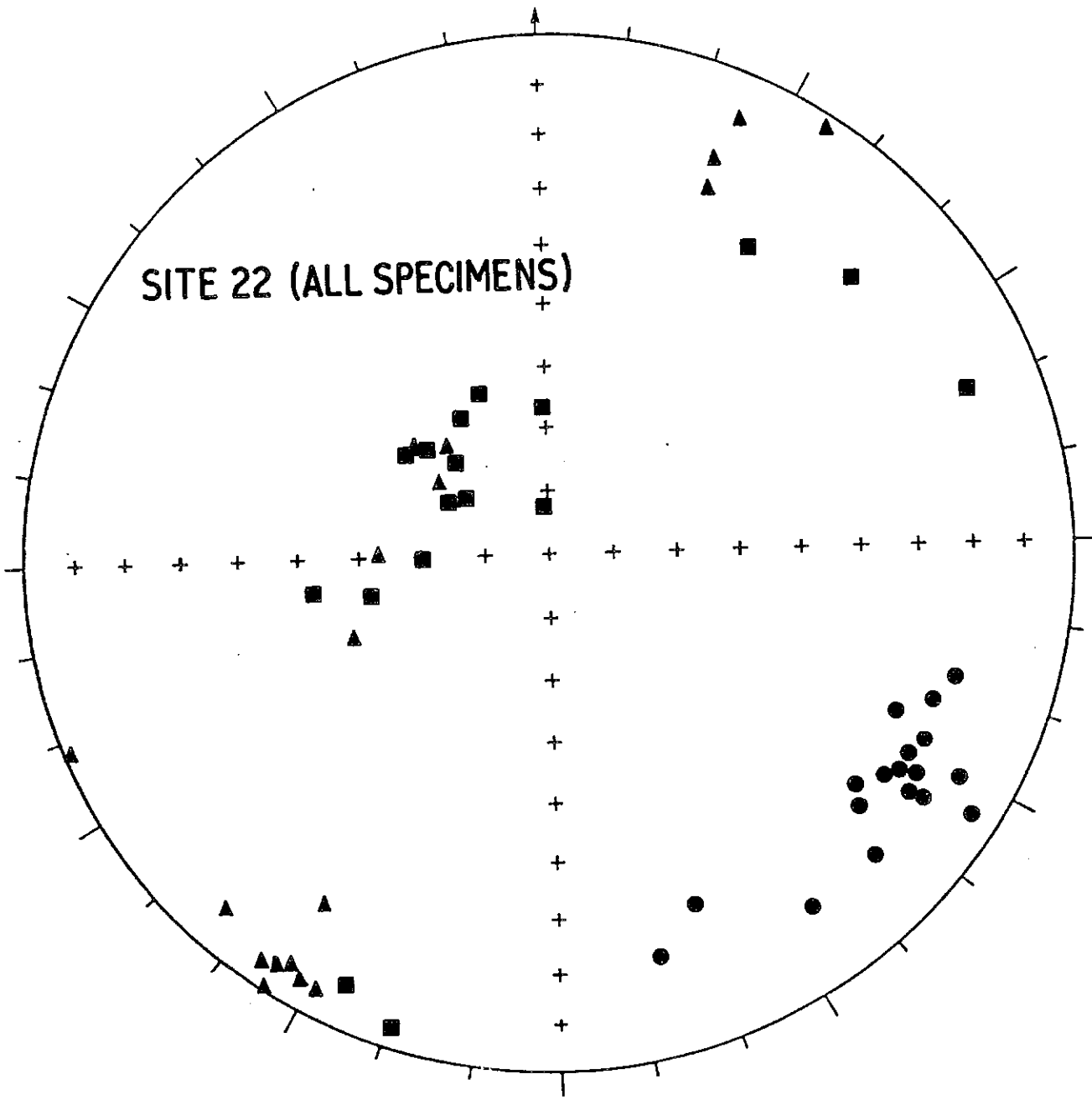

FIG. 10

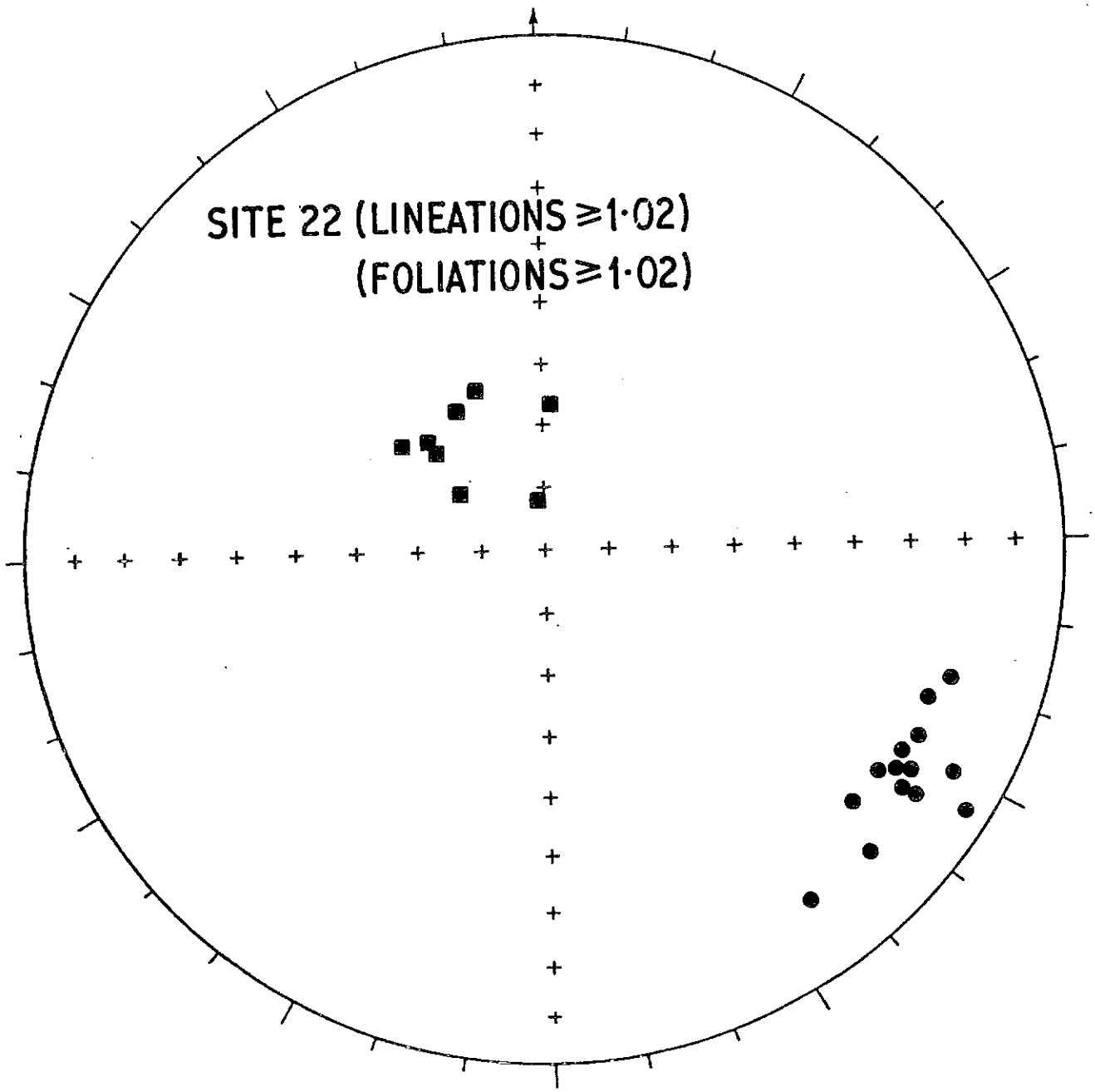

FIG.11